



THE EFFECTS OF INNER BOUNDARY LAYER THICKNESS ON THE NEAR PRESSURE FIELD OF A SUBSONIC JET

S. Meloni ^{1*}

M. Mancinelli ²

R. Camussi ²

C. Bogey ³

¹ Università della Tuscia, Department of Economics, Engineering, Society and Business Organization, Viterbo, Italy

² Università degli Studi Roma Tre, Department of Civil, Computer and Aeronautical Engineering, Rome, Italy

³ Univ Lyon, CNRS, Ecole Centrale de Lyon, INSA Lyon, Université Claude Bernard Lyon I, Ecully, France

ABSTRACT

In this work, the effects of the jet's initial conditions on the aeroacoustic properties are studied. The present investigation has been carried out using a Large Eddy Simulation (LES) database containing pressure time series covering a domain that varies in the stream-wise direction from $x=0$ up to $x/D=20$ and in the radial direction from $r/D=0.5$ (nozzle lip) up to $r/D=3$, where D is the jet exit diameter. As mentioned above, the key parameter we explored is the boundary-layer thickness (δ_{BL}), which has been varied keeping fixed the nozzle exhaust turbulence intensity at $TI = 0\%$. Specifically, the value of δ_{BL} , normalised by the nozzle radius r_0 , spans from 0.025 up to 0.4. The acoustic component of the near pressure field of the jet is extracted by applying a wavelet-based procedure to the pressure data. The decomposed signals are then analysed separately in terms of statistical quantities.

Keywords: *Aeroacoustics, Jet-Noise, Wavelet*

1. INTRODUCTION

Since the seminal work of Lighthill [1], which provided a theoretical framework for predicting the noise generated by turbulent flows, many studies have been devoted

*Corresponding author: stefano.meloni@unitus.it.

Copyright: ©2023 Meloni et al. This is an open-access article distributed under the terms of the Creative Commons Attribution 3.0 Unported License, which permits unrestricted use, distribution, and reproduction in any medium, provided the original author and source are credited.

to identifying the physical mechanisms by which jet turbulent structures generate noise (see e.g. [2–4]). In this framework, a key role is played by the state of the flow at the jet nozzle exit, which is known to influence significantly both the aerodynamic and the acoustic properties of the jet, affecting the degree of mixing between the jet and the surrounding ambient air. The initial conditions can be clustered into five main parameters: Reynolds number (Re), Mach number (Ma), shear-layer momentum defined by the boundary-layer (BL) thickness, the boundary-layer velocity profile [2–5], and the turbulence intensity (TI).

The investigation of the near pressure field is crucial for a better understanding of the noise generation mechanism. Pressure fluctuations in the near field of the jet comprise a hydrodynamic component associated with the disturbances induced by the turbulent flow structures and a propagative acoustic component radiating in the far field. The decomposition of these two pressure components is essential to develop more accurate noise prediction tools and implement noise control strategies. Different separation techniques have been presented in the literature ([5–9]).

The parametric analysis proposed herein attempts to clarify the sensitivity of the acoustic and hydrodynamic pressures (separated using the method proposed in [7]) to the initial boundary-layer thickness δ_{BL} , normalized by the nozzle exhaust radius r_0 . We explore different values of δ_{BL}/r_0 , from 0.025 to 0.4, keeping fixed the nozzle exhaust turbulence intensity at $TI = 0\%$. The investigation is focused on the region close to the jet flow where, as outlined in [5], the disturbances, destined to be-

come noise in the far field, are contained. We consider a well-detailed Large-Eddy-Simulation (LES) database (see among many [10–13]) containing pressure time series covering a domain that varies in the stream-wise direction from $x/D = 0$ to $x/D = 20$ and in the radial direction from $r/D = 0.5$ (lipline) to $r/D = 3$, where D is the jet exit diameter. The acoustic and hydrodynamic components of the pressure time series are extracted by applying a well-known procedure in the literature [7] based on the application of wavelet transform to the pressure data. The decomposed signals are then analyzed separately in terms of statistical content and directivity.

Further details on the numerical setup and the wavelet-based decomposition procedure are given in §2 and 3, respectively. The main results are reported in §. 4, whereas conclusions and final remarks are given in §.5.

2. NUMERICAL SETUP

LESs of round free jets at a Reynolds number $Re = 10^5$ and $M = 0.9$ have been used for the analysis reported in this paper. The simulations have been carried out with $TI = 0$ (fully laminar case) and normalized boundary layer thickness δ_{BL}/r_0 varying from 0.025 to 0.4. The jet initial conditions are summarized in table 1 for clarity.

M_j	Re_D	δ/r_0
0.9	10^5	0.025
0.9	10^5	0.05
0.9	10^5	0.1
0.9	10^5	0.2
0.9	10^5	0.4

Table 1: Jet initial conditions

An in-house solver, based on the three-dimensional filtered compressible Navier–Stokes equations in cylindrical coordinates, has been used to perform the LES simulations. Specifically, the LESs were carried out using grids containing a number of points varying between 250 million and 1 billion, with low-dissipation schemes and relaxation filtering as a subgrid dissipation model [14]. More information can be found in references [10–12].

3. WAVELET-BASED PROCEDURE

The separation of the acoustic and hydrodynamic components of the near-field pressure signals is achieved by

applying the procedure proposed by [7] that is briefly worked out in what follows.

The method is based on the wavelet transform of pressure signals and an appropriate filtering of the resulting wavelet coefficients performs well in identifying and isolating intermittent features within the turbulent flow, as suggested by [6]. For a pressure time series $p(t)$, the wavelet transform can be formally expressed by [15, 16],

$$w(s, t) = C_\psi^{-\frac{1}{2}} s^{-\frac{1}{2}} \int_{-\infty}^{\infty} p(\tau) \psi^* \left(\frac{t - \tau}{s} \right) d\tau, \quad (1)$$

where s is the wavelet scale, τ is a time shift, $C_\psi^{-\frac{1}{2}}$ is a constant that takes into account the mean value of $\psi(t)$ and $\psi^* \left(\frac{t - \tau}{s} \right)$ is the complex conjugate of the dilated and translated mother wavelet $\psi(t)$.

With the aim of performing the acoustic/hydrodynamic separation, the wavelet coefficients can be separated by assuming that the hydrodynamic contribution, being related to localized eddy structures, compresses well onto the wavelet basis so that it originates, in the transformed domain, few but large-amplitude wavelet coefficients. Thus, the so-called pseudo-sound (i.e., the hydrodynamic component of pressure fluctuations) can be extracted by selecting the wavelet coefficients exceeding a proper threshold. In the present approach, the threshold is identified by applying the 'WT3' technique presented in [7] and applied successfully to other flow phenomena other than jet noise [17–19]. We remind the reader that the method is based on single-point statistics and, hence, requires only pointwise signals from single virtual probes [20].

In summary, the procedure splits a given pressure signal into two-time series representing the acoustic and the hydrodynamic pressure components. The two-time series are then processed separately with the aim of characterising their statistical properties.

An example in the Fourier domain of a decomposed signal is reported in figure 1 for $x/D = 4$ and $r/D = 1$. It is shown that the hydrodynamic component contains most of the signal low-frequency energy content, whereas the acoustic pressure is dominant at high frequencies.

4. RESULTS

The results are presented in terms of Overall Sound Pressure Level (*OASPL*), which is defined as follows:

$$OASPL = 20 \log_{10} \left(\frac{\sigma}{p_{\text{ref}}} \right), \quad (2)$$

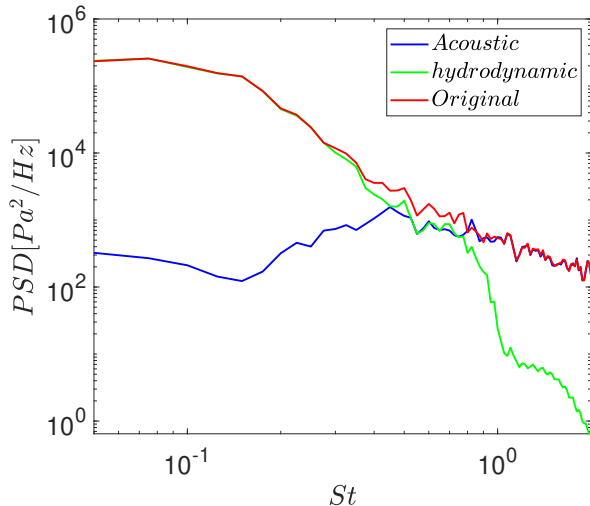


Figure 1: Decomposed pressure spectra, at $x/D=8$, $r/D=2$ and $\delta_{BL} = 0.05$

where σ is the standard deviation of the pressure signal and p_{ref} is a reference pressure whose value is $20\mu Pa$.

Figure 2 reports the OASPL of the acoustic pressure for different boundary layer thicknesses. The BL thickness mostly affects the acoustic pressure directivity. Specifically, the noise emission is in the sideline direction for low δ/r_0 and moves to shallow polar angles for increasing BL thicknesses. The different noise directivity pattern is likely related to the growth rate and saturation region in the streamwise direction of the Kelvin-Helmholtz instability that are both affected by the shear-layer thickness, which is likewise strongly influenced by the inner BL thickness.

The significant role played by the BL/shear-layer thickness in the jet noise directivity pattern is confirmed by the hydrodynamic field reported in figure 3. We note that the pseudo-sound component appears to be substantially affected by the BL thickness mainly in the jet shear layer for large thickness values (e.g. $\delta/r_0 > 0.1$). Further analyses have to be carried out to physically interpret the trends presented herein.

5. CONCLUSIONS

In the present paper we investigated the influence of the nozzle exit boundary layer thickness of a compressible subsonic jet on the near-field hydrodynamic and acous-

tic pressures. The investigation is performed by processing a numerical database obtained by well-resolved LES at fixed Mach and Reynolds numbers. The cases explored herein correspond to initial laminar conditions. The acoustic pressure component is extracted from the pressure time series by applying an existing wavelet-based procedure. It is observed that the boundary layer thickness significantly influences the noise directivity. Specifically, the maximum sound emission moves from sideline to shallow polar angles for increasing BL thicknesses, whereas the hydrodynamic component is enhanced in the shear layer region for larger BL thicknesses.

6. ACKNOWLEDGMENTS

C. Bogey was partially supported by the LABEX CeLyA (ANR-10-LABX-0060/ANR-16-IDEX-0005).

The numerical data analyzed in this work were obtained using the HPC resources of PMCS2I (Pôle de Modélisation et de Calcul en Sciences de l'Ingénieur et de l'Information) of Ecole Centrale de Lyon and P2CHPD (Pôle de Calcul Hautes Performances Dédié) of Université Lyon I, and the resources of CINES (Centre Informatique National de l'Enseignement Supérieur) and IDRIS (Institut du Développement et des Ressources en Informatique Scientifique) under the allocation 2021-2a0204 made by GENCI (Grand Equipement National de Calcul Intensif).

7. REFERENCES

- [1] M. J. Lighthill, "On sound generated aerodynamically," *General theory. Proc. R. Soc. Lond.*, pp. 564–587, 1952.
- [2] M. E. Goldstein, "Aeroacoustics of turbulent shear flows," *Annu. Rev. Fluid Mech.*, vol. 16, no. 1, pp. 263–285, 1984.
- [3] G. Lilley, "On the noise from air jets.," *AGARD CP 131*, pp. 13.1–13.2, 1974.
- [4] A. V. G. Cavalieri, P. Jordan, A. Agarwal, and Y. Gervais, "Jittering wave-packet models for subsonic jet noise," *J. Sound Vib.*, vol. 330, no. 18-19, pp. 4474–4492, 2011.
- [5] C. E. Tinney and P. Jordan, "The near pressure field of co-axial subsonic jets," *Journal of Fluid Mechanics*, vol. 611, p. 175–204, 2008.

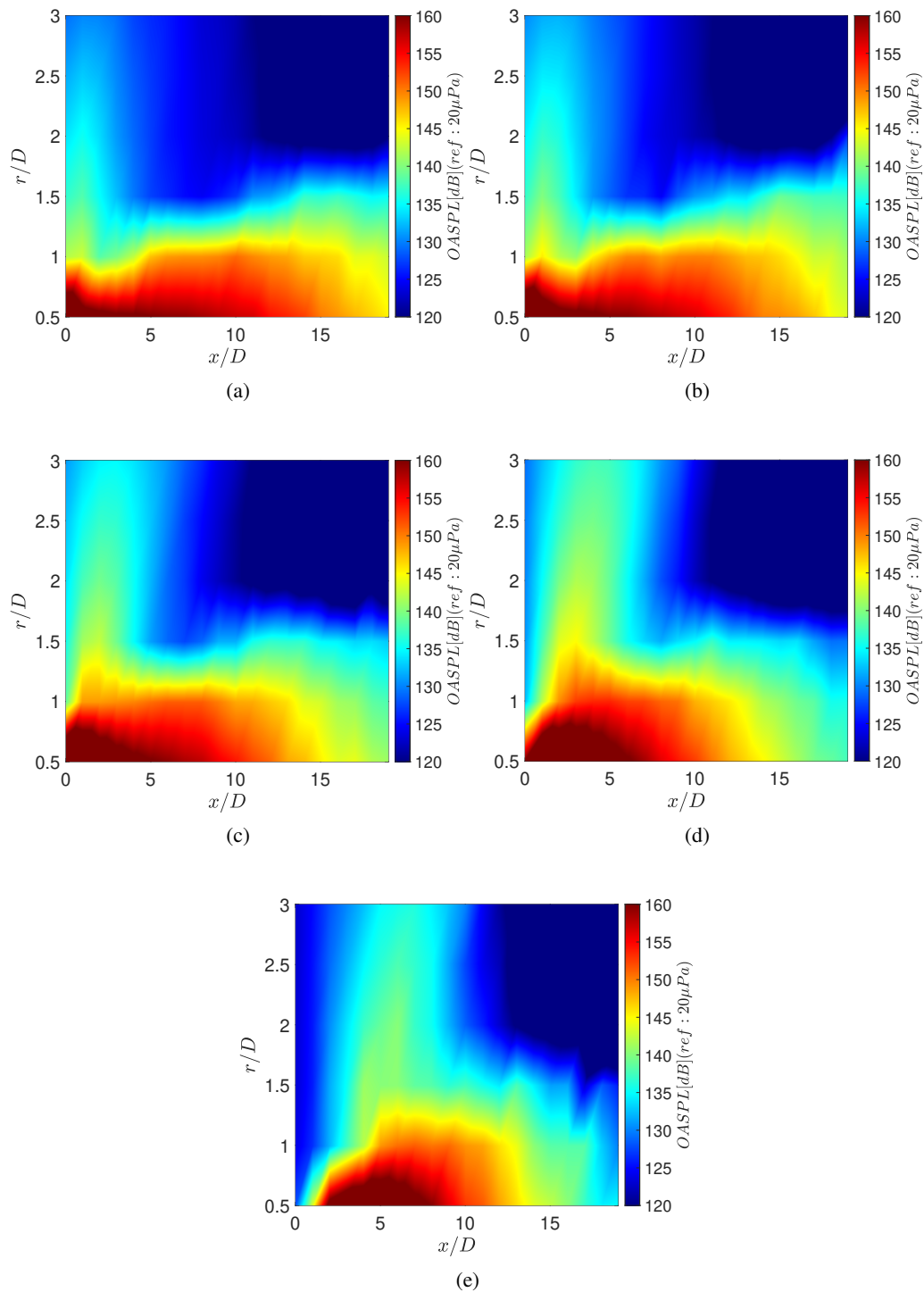


Figure 2: OASPL acoustic maps for different nozzle exhaust boundary layer thicknesses: a) $\delta/r_0 = 0.025$; b) $\delta/r_0 = 0.05$; c) $\delta/r_0 = 0.1$; d) $\delta/r_0 = 0.2$; e) $\delta/r_0 = 0.4$.

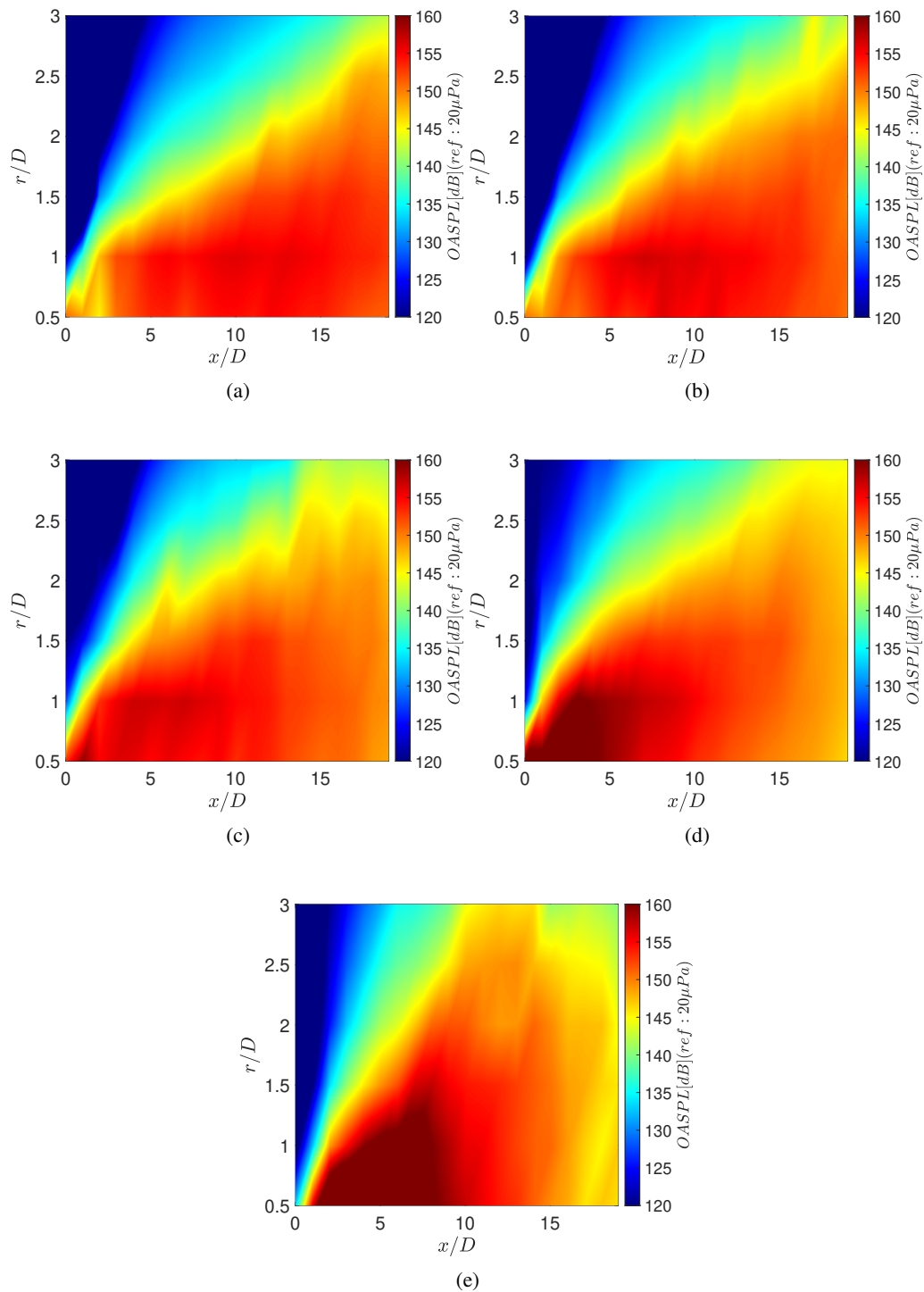


Figure 3: OASPL hydrodynamic maps for different nozzle exhaust boundary layer thicknesses: a) $\delta/r_0 = 0.025$; b) $\delta/r_0 = 0.05$; c) $\delta/r_0 = 0.1$; d) $\delta/r_0 = 0.2$; e) $\delta/r_0 = 0.4$.

- [6] S. Grizzi and R. Camussi, “Wavelet analysis of near-field pressure fluctuations generated by a subsonic jet,” *Journal of Fluid Mechanics*, vol. 698, pp. 93–124, 2012.
- [7] M. Mancinelli, T. Pagliaroli, A. Di Marco, R. Camussi, and T. Castelain, “Wavelet decomposition of hydrodynamic and acoustic pressures in the near field of the jet,” *Journal of Fluid Mechanics*, vol. 813, pp. 716–749, 2017.
- [8] M. Mancinelli, T. Pagliaroli, R. Camussi, and T. Castelain, “On the hydrodynamic and acoustic nature of pressure proper orthogonal decomposition modes in the near field of a compressible jet,” *J. Fluid Mech.*, vol. 836, pp. 998–1008, 2018.
- [9] H. K. Jawahar, S. Meloni, and R. Camussi, “Jet noise sources for chevron nozzles in under-expanded condition,” *International Journal of Aeroacoustics*, vol. 0, no. 0, p. 1475472X221101766, 0.
- [10] C. Bogey, “Interactions between upstream-propagating guided jet waves and shear-layer instability waves near the nozzle of subsonic and nearly ideally expanded supersonic free jets with laminar boundary layers,” *Journal of Fluid Mechanics*, vol. 949, p. A41, 2022.
- [11] C. Bogey, “A database of flow and near pressure field signals obtained for subsonic and nearly ideally expanded supersonic free jets using large-eddy simulations.” <https://hal.archives-ouvertes.fr/hal-03626787>, 2022.
- [12] C. Bogey, “Generation of excess noise by jets with highly disturbed laminar boundary-layer profiles,” *AIAA Journal*, vol. 59, no. 2, pp. 569–579, 2021.
- [13] R. Camussi, S. Meloni, and C. Bogey, “On the influence of the nozzle exhaust initial conditions on the near field acoustic pressure,” *Acta Acust.*, vol. 6, p. 57, 2022.
- [14] C. Bogey, O. Marsden, and C. Bailly, “Large-eddy simulation of the flow and acoustic fields of a reynolds number 10^5 subsonic jet with tripped exit boundary layers,” *Physics of Fluids*, vol. 23, p. 035104, 2011.
- [15] M. Farge, “Wavelet transform and their applications to turbulence,” *Annual Review of Fluid Mechanics*, vol. 24, no. 1, pp. 395–458, 1992.
- [16] R. Camussi, G. Robert, and M. C. Jacob, “Cross-wavelet analysis of wall pressure fluctuations beneath incompressible turbulent boundary layers,” *Journal of Fluid Mechanics*, vol. 617, p. 11–30, 2008.
- [17] S. Li, D. E. Rival, and X. Wu, “Sound source and pseudo-sound in the near field of a circular cylinder in subsonic conditions,” *Journal of Fluid Mechanics*, vol. 919, p. A43, 2021.
- [18] A. Hajczak, L. Sanders, F. Vuillot, and P. Druault, “Wavelet-based separation methods assessment on the near pressure field of a landing gear subcomponent,” in *25th AIAA/CEAS Aeroacoustics Conference*, p. 2482, 05 2019.
- [19] C. Pérez Arroyo, G. Daviller, G. Puigt, C. Airiau, and S. Moreau, “Identification of temporal and spatial signatures of broadband shock-associated noise,” *Shock Waves*, vol. 29, no. 1, pp. 117–134, 2019.
- [20] R. Camussi and S. Meloni, “On the application of wavelet transform in jet aeroacoustics,” *Fluids*, vol. 6, no. 8, p. 299, 2021.